

# Update to the ACIS Contamination Model

January 8, 2010

## 1 Introduction

ACIS observations of astronomical sources as well as its own external calibration source (ECS) have shown that molecular contamination has been building up on the optical/UV blocking filters since launch. Early LETG/ACIS observations of Ton S180 in Nov. 1999 and 3C 273 in Jan. 2000 showed that there was a slight reduction in the low energy ACIS QE<sup>1</sup>. A near-simultaneous LETG/HRC-S observation of 3C273 did not show a similar problem with the low energy HRC-S QE. It was not clear that the low energy QE was systematically decreasing with time until a deep LETG/ACIS-S observation of Mkn 421 in 2002 showed an even further reduction in the low energy QE and the presence of absorption edges produced by C, O and F. Since ACIS operates at a focal plane temperature of -120 ° and the HRC operates at roughly room temperature, it was concluded that the reduction in the low energy QE of ACIS was due to out gassed material condensing on the cold ACIS filters. The composition of the molecular contaminant on the ACIS filters is discussed in detail in Marshall et al. (2004).

During the first few weeks after launch, the charge transfer inefficiency (CTI) of the ACIS CCDs increased significantly due to radiation damage incurred during passage through the Earth's radiation belts near perigee. Since that time, ACIS is stowed during each perigee pass, i.e., the HRC is at the focal point. When ACIS is stowed, it is illuminated by its ECS, which consists of a bare Fe55 source, an Al fluorescence source and a Ti fluorescence. To monitor the build-up of contamination on the ACIS filters, data is collected from the ECS before and after each perigee pass. To provide sufficient statistics, the ECS data must be co-added into 3 month intervals.

The ECS has a strong Mn-K line at 5.9 keV and Mn-L and F-K lines that comprise most of the line emission around 660 eV (see Fig. 1). This figure shows a calorimeter resolution spectrum of an Fe55 source that was kindly provided to the Chandra calibration team by Dan McCammon<sup>2</sup>. With the energy resolution of the ACIS CCDs, the Mn-L and F-K lines are blended into a single feature near 660 eV. Prior to 2009, only a CCD resolution spectrum of the ECS was available to the calibration team and it was assumed that the blended feature near 660 eV was primarily due to emission from Mn-L and Fe-L emission lines<sup>3</sup>. Since the Mn-K  $\alpha$  line at 5.9 keV is not affected by absorption, the optical depth of the contaminant can be monitored by measuring the flux ratio between the blended lines at 660 eV and the Mn-K  $\alpha$  line. Since the individual lines near 660 eV cannot be resolved with the ACIS CCDs, a flux weighted opacity must be computed based on a model for the line energies and relative line strengths. Prior to 2009, this was done assuming the emission was dominated by Mn-L and Fe-L emission lines. Since that time, the emission lines and line strengths shown in Fig. 1 have been used. The ECS data also provides information on the optical depth at the Al-K  $\alpha$  (1.49 keV) fluorescence line. The optical depth at Ti-K  $\alpha$  (4.51 keV) is simply too low to be measured reliably.

---

<sup>1</sup>see H. Marshall's memo at [http://space.mit.edu/ASC/calib/letg\\_acis/ck\\_cal.html](http://space.mit.edu/ASC/calib/letg_acis/ck_cal.html)

<sup>2</sup>see A. Besemer's memo at <http://www.astro.wisc.edu/besemer/research.html>

<sup>3</sup>see A. Vikhlinin's memo at [http://hea-www.harvard.edu/alexey/acis/memos/cont\\_spat.pdf](http://hea-www.harvard.edu/alexey/acis/memos/cont_spat.pdf)

The ECS data shows that the contaminant is not uniformly distributed across the ACIS-I and ACIS-S filters. For both detectors, the thickness of the contaminant increases towards the edges of the filters<sup>3</sup>. In addition to the ECS data, LETG/ACIS-S observations of either PKS2155-304 or Mkn421 have been carried-out semi-annually since 2002. The gratings observations measure the optical depth at the C, O and F-K edges at the nominal gratings positions. There have also been some LETG/ACIS-S calibration observations near the read-out of ACIS-S where the contaminant is thicker to measure the spatial variations in the optical depth at the C, O and F-K edges.

From early gratings observations, it was apparent that a spectral model based solely on absorption from H, C, O and F could not reproduce the observed spectral features of the ACIS contaminant. Using a model with just absorption by these elements, normalized by the observed optical depths at their K-edges, under predicted the absorption of the contaminant at 660 eV as measured by the ECS data. A two-level (or fluffium) model was adopted as an extra spectral component<sup>4</sup>. The physical justification for such an extra component is the likelihood that the contaminant is not a perfectly smooth slab of material on the filters, but has some surface roughness, or distribution of thicknesses. Due to the presence of surface roughness, different regions, or different optical depths of the contaminant are sampled at different energies. Just above an atomic edge, where the material is the most optically thick, the measurement is heavily weighted by photons that pass through the thinnest portions of the contaminant. Just below an atomic edge, the measurement is more evenly weighted by photons passing through both physically thick and thin regions. A similar two-level model was used to model the effects of ice on the *Einstein* SSS.

## 2 Previous ACIS Contamination Models

The first calibration product that was released to account for the effects of contamination on the ACIS filters was an alternative ACIS-S QE to be used solely with LETG/ACIS-S data. This alternative QE was released to the users in CALDB 2.6 on June 1, 2001. Since that time, the ACIS contamination model has been incorporated into a separate calibration product which can be applied to all ACIS data. There have been two prior releases of the ACIS contamination model. Version N0003 was released in CALDB 2.26 on Feb. 2, 2004. That version assumed a uniform layer of contaminant on both the ACIS-I and ACIS-S filters. Version N0004 was released in CALDB 3.0 on Dec. 14, 2004. That version included an adjustment for the spatial variations in the depth of the contaminant across the ACIS filters. Due to the lack of gratings data on ACIS-I, the composition of the contaminant was assumed to be the same on both the ACIS-I and ACIS-S filters with ratios of C:O=14 and C:F=11.5 as derived from the LETG/ACIS-S data. A two-level (fluffium) model was also used in these early versions of the ACIS contamination model. The two-level model assumed that there were only two distinct thicknesses for the contaminant. The two-level model which produced the best fit with the ECS data has optical depths of 5.7 and 0.97 with filling factors of 15% and 85% for the thick and thin regions, respectively<sup>4</sup>. The spectral and time-dependence of the ACIS contamination model was then derived by matching the elemental model only (i.e., just the absorption by C, O and F) to the measured optical depth at the C-K edge. This elemental model was then used to predict the optical depth at 660 eV as

---

<sup>4</sup>see D. Dewey's memo at [space.mit.edu/HETG/technotes/contam/twolevel.html](http://space.mit.edu/HETG/technotes/contam/twolevel.html)

measured by the ECS. The difference in predicted and measured optical depth at 660 eV was then accounted for by adding in the appropriate amount of fluffium.

The depth of the contaminant on the ACIS-S filter has been found to be fairly uniform along the ACIS-S array (i.e., in the chipx or dispersion direction) and increases toward the top and bottom of the filter. The ECS data were used to fit an analytic function to the optical depth of the contaminant as a function of chipy only for ACIS-S. For ACIS-I, the ECS data showed that the optical depth of the contaminant was approximately azimuthally symmetric about the center of the detector and the optical depth was modeled as an analytic function based solely on the distance from the center of the detector. In version N0004, the spatial shape of the contaminant was assumed to be time-independent (see the memo by A. Vikhlinin for details<sup>3</sup>).

### 3 Updated ACIS Contamination Model

Version N0004 provided a good fit to the ECS data up until about 2006 (see Fig. 2). This figure shows that the optical depth of the contaminant predicted by version N0004 underestimates the optical depth derived from the ECS data after this time. This figure also shows that the time dependence of the contamination build-up changed around 2005. Fig. 3 shows the discrepancy between the measured optical depth at the C-K from LETG/ACIS-S observations of blazars and the predictions of version N0004.

#### 3.1 ACIS-S Contamination Model

A major change to the new contamination model is an adjustment in the time dependence to account for the accelerated build-up of contaminant relative to extrapolations from version N0004 of the contamination model (see Fig. 4). Also, the improved gain corrections for the S1 and S3 chips (released in CALDB 3.4.3 on March 31, 2008) at a focal plane temperature of  $-110^{\circ}$  (the ACIS operating temperature during the first 3 months after launch), permit a more accurate measurement of the contamination buildup early in the Chandra mission. A simple extrapolation of the ECS-measured optical depths taken during the Chandra mission imply an optical depth of approximately 0.1 just after launch (see Figs. 4 and 5). This is highly unlikely because ACIS was warm prior to launch. Figure 4 also shows that a rising exponential with  $\tau = 0$  fixed at launch (red dashed line) does not provide as good a fit to the ECS data. A zero-point offset of approximately 0.1 in the ECS-measured optical depth is marginally consistent with the uncertainties of the pre-launch ECS measurement and was used in generating version N0005 of the ACIS-S contamination model.

Another change is the inclusion of a new energy dependence for the absorption of the contaminant in excess of the purely elemental model. As stated above, a two-level (fluffium) model was used for versions N0003 and N0004 of the ACIS contamination model to produce agreement between the gratings measured optical depths at the atomic K-edges and the ECS-measured optical depth at 660 eV. An alternative approach, implemented in this new release, features an empirical determination of the extra absorption component. This was done by taking the ratio of a 2009 ACIS-S3 spectrum of the Coma cluster to a 1999 ACIS-S3 spectrum. After taking into account the elemental absorption, the ratio of Coma spectra shows an additional

component whose optical depth gradually increases toward lower energies. The extra component can be adequately fit by a Gaussian centered at  $E=0$  and  $\sigma = 600$  eV. This component was adopted in the generation of version N0005 of the ACIS-S contamination model. The ratio of the absorption in the individual elements (C, O, F) and the additional component was measured using LETG spectra of AGNs. The results indicate that, within the uncertainties, the spectrum of the additional absorption component has not changed over the past 10 years, and hence, can be normalized at any point in time and location on ACIS-S using the ECS measurements.

The final update includes a different method for modeling the spatial variation in the depth of the contaminant on ACIS-S. Figure 6 shows the difference between the ECS measured optical depths at the top and bottom of ACIS-S and the optical depth at the center of ACIS-S. Version N0005 of the ACIS-S contamination model uses the analytic function shown as a solid line in Fig. 6 to compute the spatial variation in the depth of the contaminant.

### 3.2 ACIS-I Contamination Model

Version N0005 of the ACIS-I contamination model uses separate analytic functions to model the time-dependence of the elemental and two-level (fluffium) components<sup>5</sup>. The elemental ratios in N0005 have been revised from version N0004 based on the average ratios measured over the course of the Chandra mission from gratings data and are now C:F = 20 and C:O = 12.5<sup>6</sup>. The same two-level model is used in version N0005 as that in N0004 for the ACIS-I contamination model. Figure 7 shows the optical depth at 660 eV as measured from the ECS data along with the predictions of an elemental model and an elemental plus fluffium model (version N0005) for the center and periphery of ACIS-I. Figure 8 shows a similar plot for the optical depth at the AL-K $\alpha$  fluorescence line.

## 4 Comparison of Versions N0004 and N0005

The oxygen rich supernova remnant E0102-72 has been observed at least once per year since launch to monitor the low energy gain and QE of the ACIS CCDs. Fig. 9 shows the 0.3-1.16 keV flux in these observations derived with version N0004 of the ACIS-S contamination model. The blue data points were done in full-frame mode and the red data points were done with a sub-array. The fluxes for the sub-array measurements are slightly higher due to pile-up. Notice that there is some time dependence to the derived fluxes, especially a 10% decrease over the past few years in the sub-array measurements. Fig. 10 shows the same data with fluxes derived using version N0005 of the ACIS-S contamination model. Notice that the full-frame and sub-array fluxes are less time-dependent.

Figure 11 shows the ACIS-S spectrum from a 1999 observation of the Coma cluster. The solid curve is the best-fit absorbed single temperature model with the absorption fixed to the galactic value. Figure 12 shows the ACIS-S spectrum from a 2009 observation of the Coma cluster using the same extraction region as that used for the 1999 spectrum. The solid curve is the best-fit model to the 1999 spectrum using version N0004 of the ACIS-S contamination model. Notice the 10% deficit below 1 keV due to the underestimate in the depth of the absorption at recent times in the N0004 model. Fitting the 2009 spectrum using the N0004 model

---

<sup>5</sup>see H. Marshall's memo at <http://space.mit.edu/ASC/calib/ContamModelv1.pdf> for details

<sup>6</sup>See H. Marshall's CCW presentation at <http://cxc.harvard.edu/ccw/proceedings/2007/presentations/marshall>

with  $N_H$  treated as a free parameter gives an excess absorption above the galactic value of  $\sim 2.0 \times 10^{20} \text{ cm}^{-2}$ . Figure 13 shows the same 2009 ACIS-S spectrum and model derived using the N0005 version of the ACIS contamination model. Notice the significant improvement in the fit below 1 keV. Table 1 shows the results of fitting a sample of 12 groups and clusters to a single temperature model for versions N0004 and N0005 of the ACIS contamination model.

Figure 14 shows the spectrum of an LETG/ACIS-S observation of Mkn 421 fitted to an absorbed power-law model using version N0004 of the ACIS contamination model. Figure 15 shows the same spectrum fitted to an absorbed power-law model using version N0005 of the ACIS contamination model. Notice the significant improvement across the C-K edge. Table 2 shows the results of fitting a sample of AGN using version N0004 and N0005 of the ACIS contamination model.

## 5 Caveats

### 5.1 Residuals near the C-K edge in LETG/ACIS-S spectra

The deep LETG/ACIS-S observation of Mkn 421 shows that there are residuals up to 0.5 optical depths in the  $43.2\text{-}43.5\text{\AA}$  (0.285-0.287 keV) band using version N0005 of the ACIS-S contamination model (see Fig. 15). This  $0.3\text{\AA}$  range samples the resolved C-K edge and the user is advised to filter out this region with high S/N LETG/ACIS-S data.

### 5.2 Low energy residuals in ACIS imaging data.

There can be 5-10% residuals in ACIS imaging data below 0.8 keV using version N0005 of the ACIS contamination model (see the plot to the 2009 Coma spectrum in Fig. 10).

## 6 References

Marshall, H., Tennant, A., Grant, C., Hitchcock, A., O'Dell, S., Plucinsky, P. 2004, SPIE, 5165, 497.

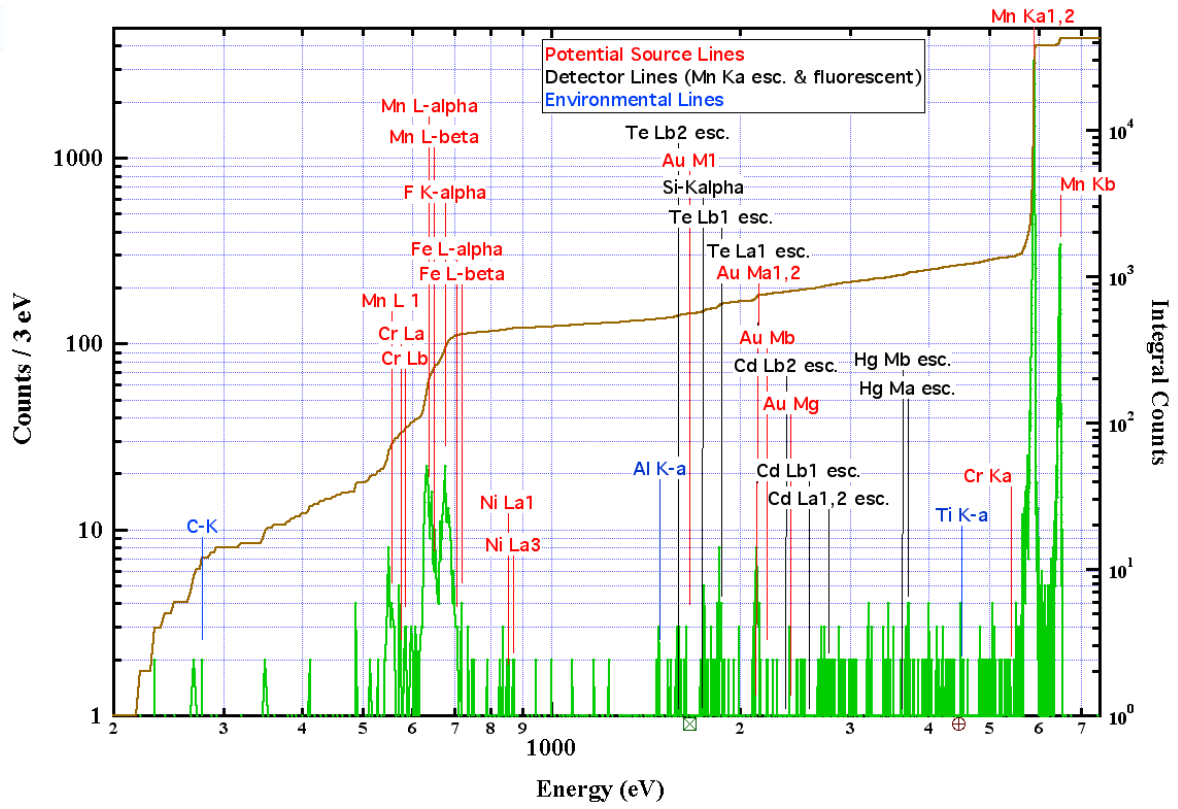


Figure 1: The spectrum of the ACIS external calibration source (ECS) provided by Dan McCammon.

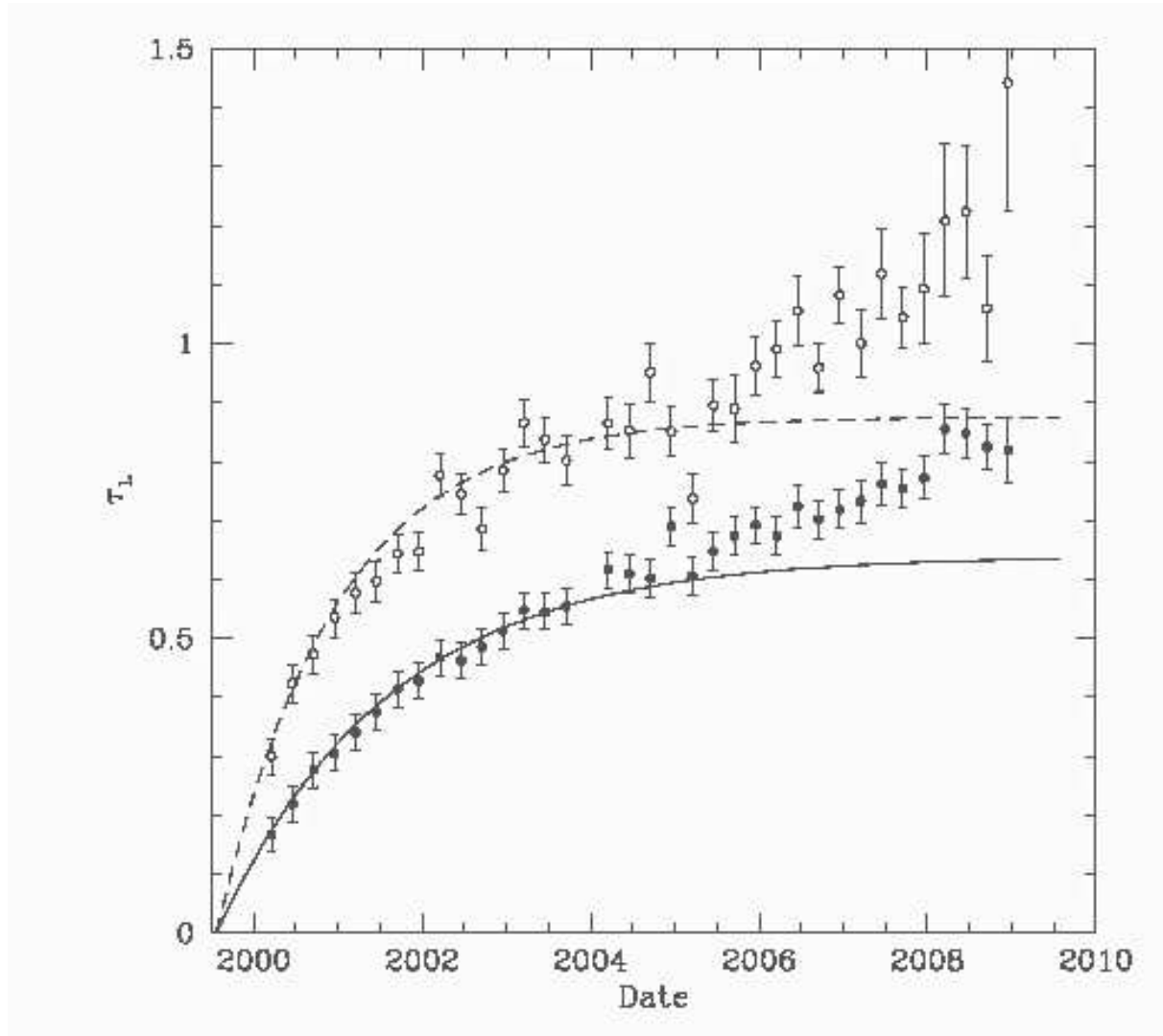


Figure 2: Optical depth at 660 eV on S3 as a function of time as measured by ECS data. The lower (solid) data points show the optical depth measured in the center of S3 and the upper (open) data points show the optical depth measured near the bottom of S3. The lines give the predictions from version N0004 of the ACIS contamination model.

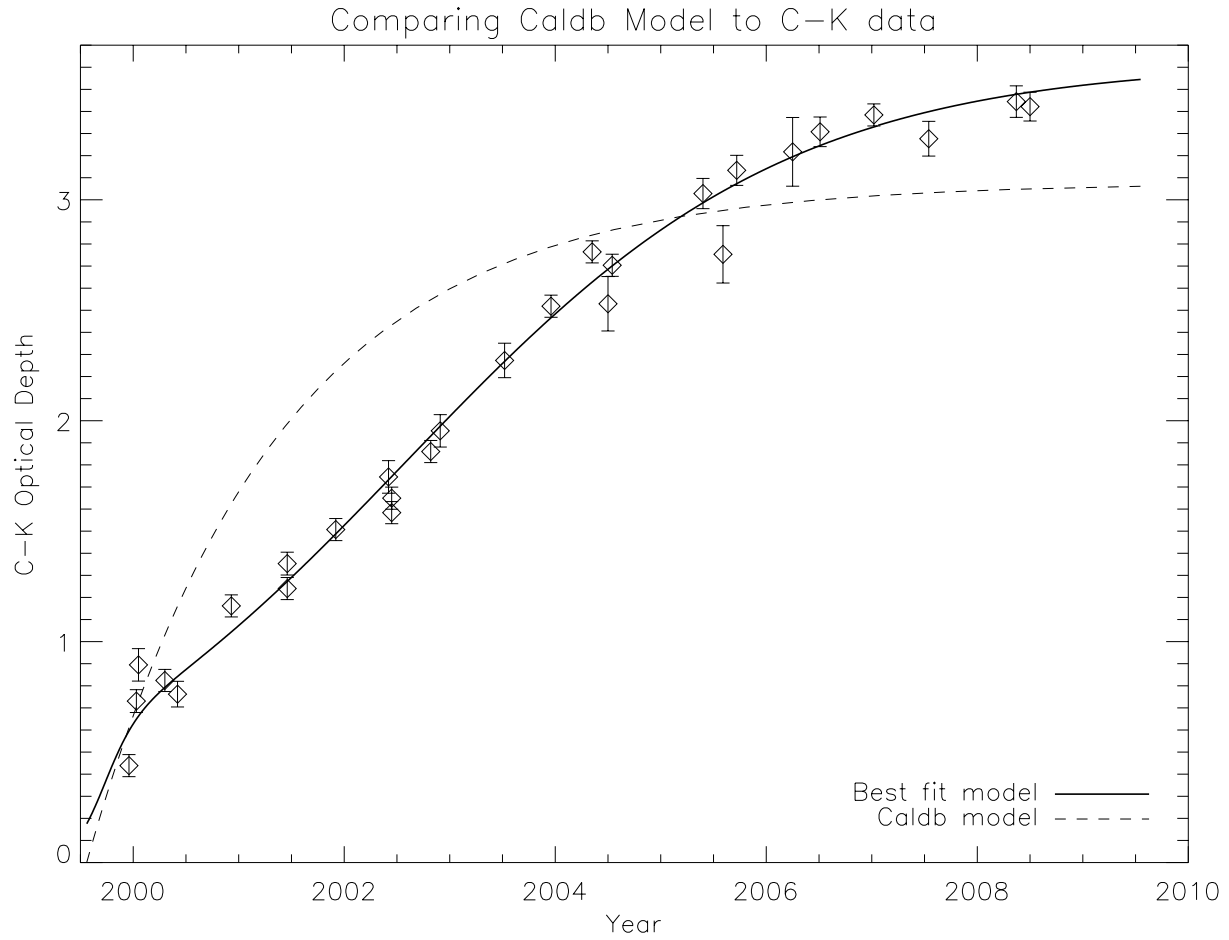


Figure 3: Measurements of the optical depth at the C-K edge from LETG/ACIS-S observations of blazars, compared to the predicted edge depth using CALDB version N0004 of the ACIS contamination model (dashed line). For a typical galactic  $N_{\text{H}}$  to one of these blazars, the optical depth at C-K would be about 0.10.

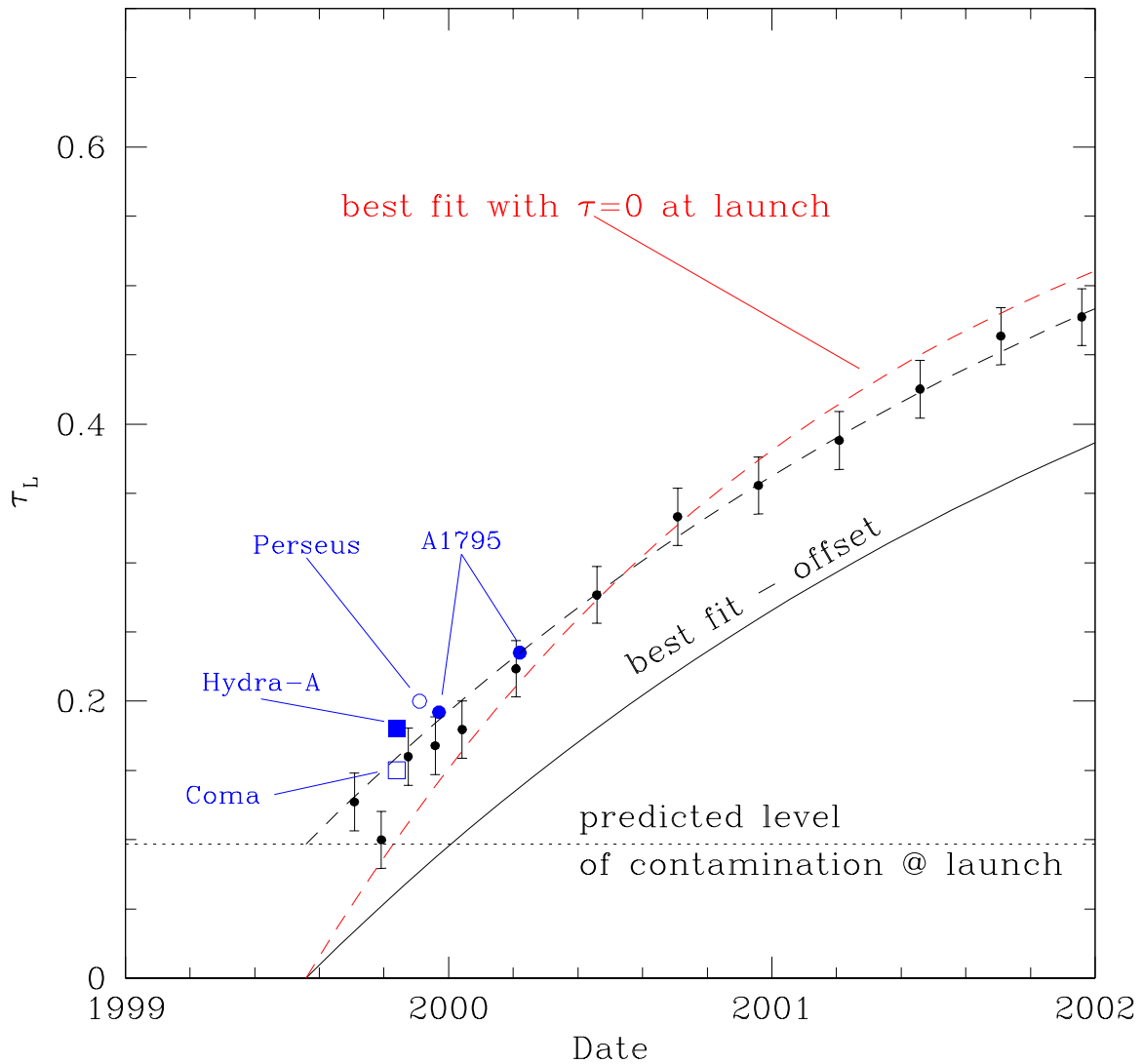


Figure 4: The black dashed line shows a fit to the ECS measured optical depths with a free value for the optical depth at launch. The red dashed line is the best-fit rising exponential with  $\tau = 0$  fixed at launch. The solid black line is off-set from the dashed black line by 0.1 and is the model used for version N0005 of the ACIS-S contamination model. The blue data points are optical depths derived from ACIS-S observations of clusters of galaxies.

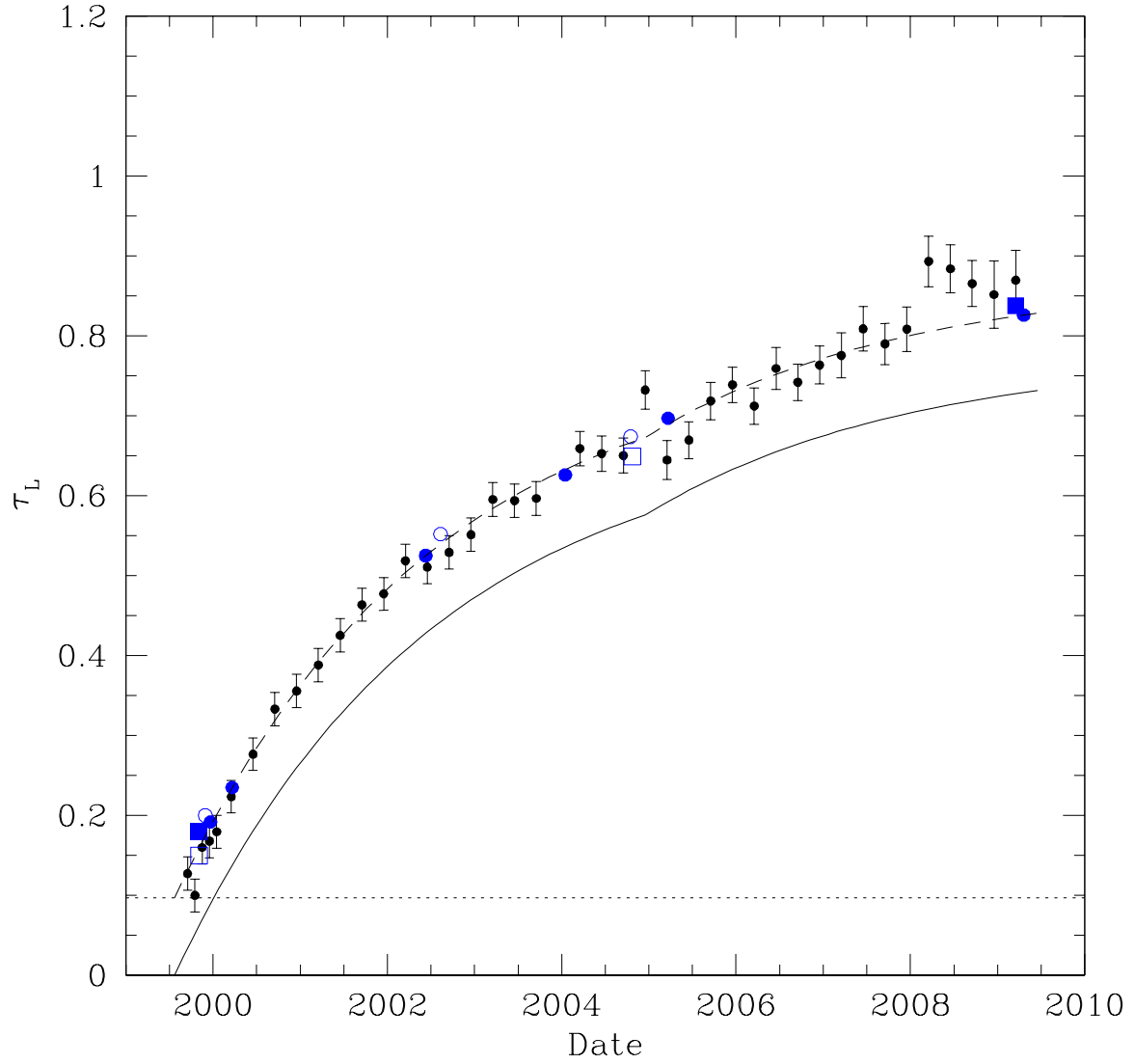


Figure 5: The time dependence used for version N0005 of the ACIS-S contamination model over the course of the mission.

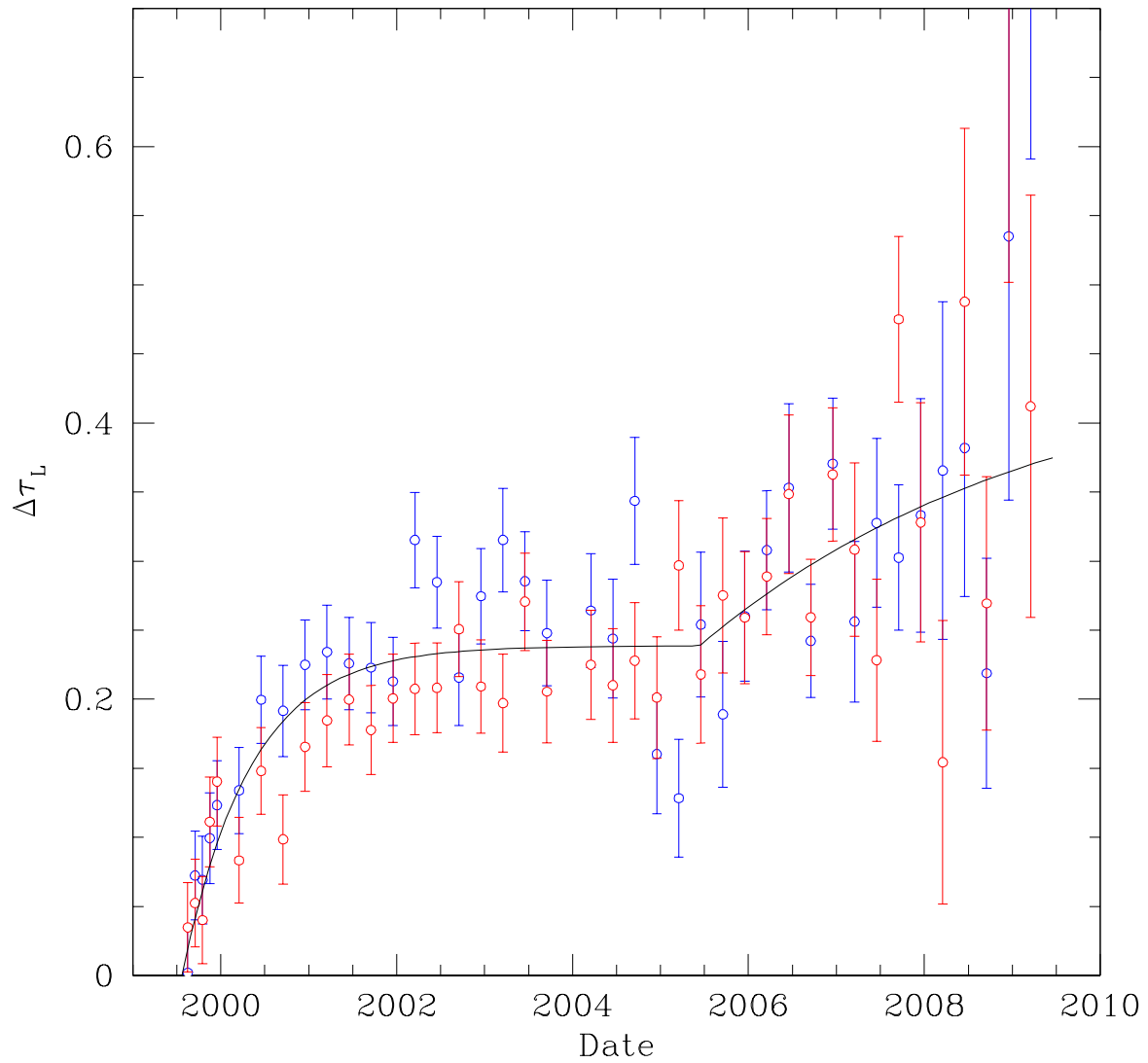


Figure 6: The difference ( $\Delta\tau$ ) between the ECS measured optical depths at the top (red data points) and bottom (blue data points) of ACIS-S and the optical depth at the center of ACIS-S. The solid line is the model used for version N0005 of the ACIS-S contamination model.

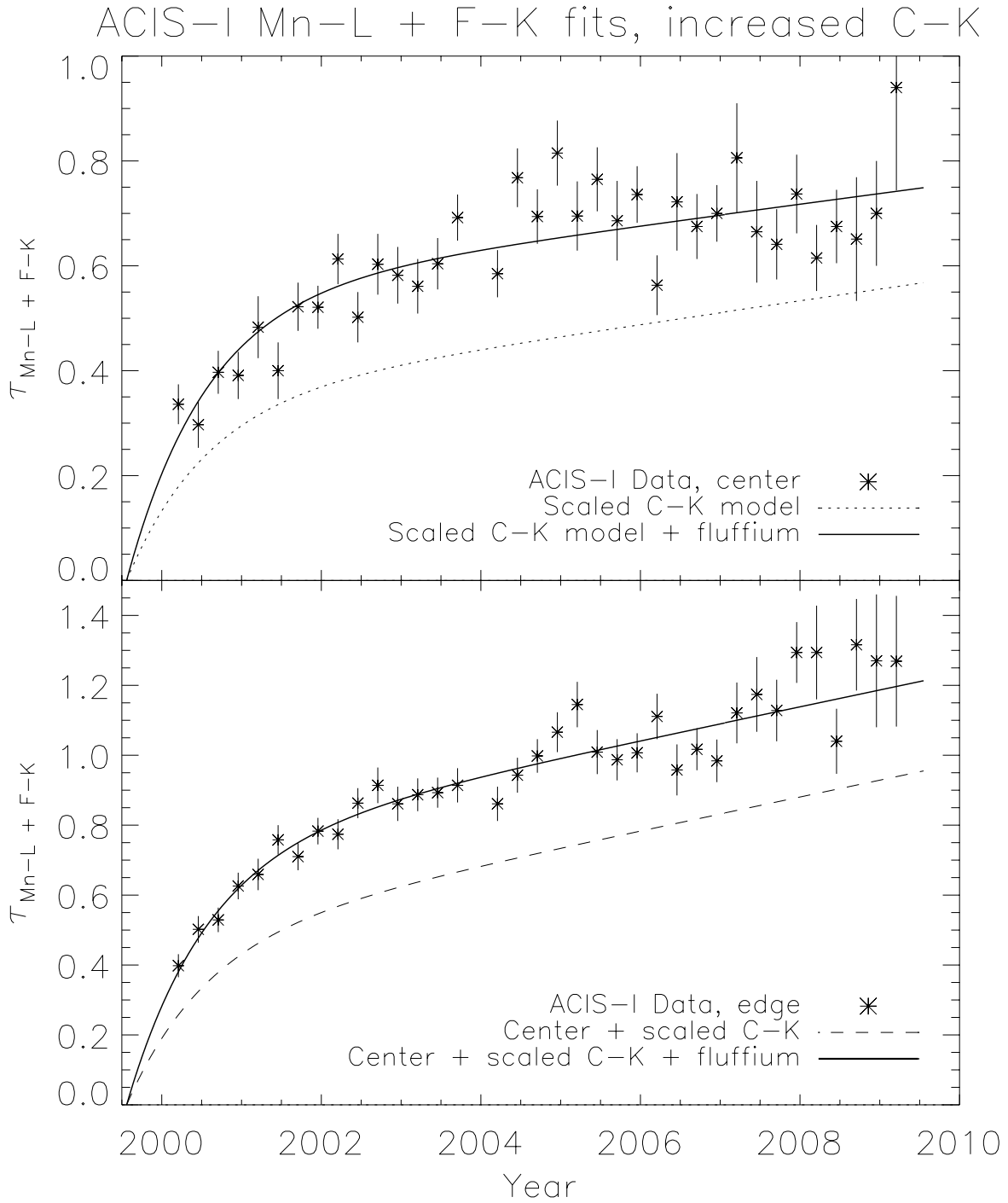


Figure 7: Optical depth at 660 eV as measured from the ECS data at the center (top plot) and periphery (bottom plot) of ACIS-I. The dashed line is the predicted optical depth assuming only absorption by C, O and F. The solid line includes both elemental and fluffium contributions to the total absorption.

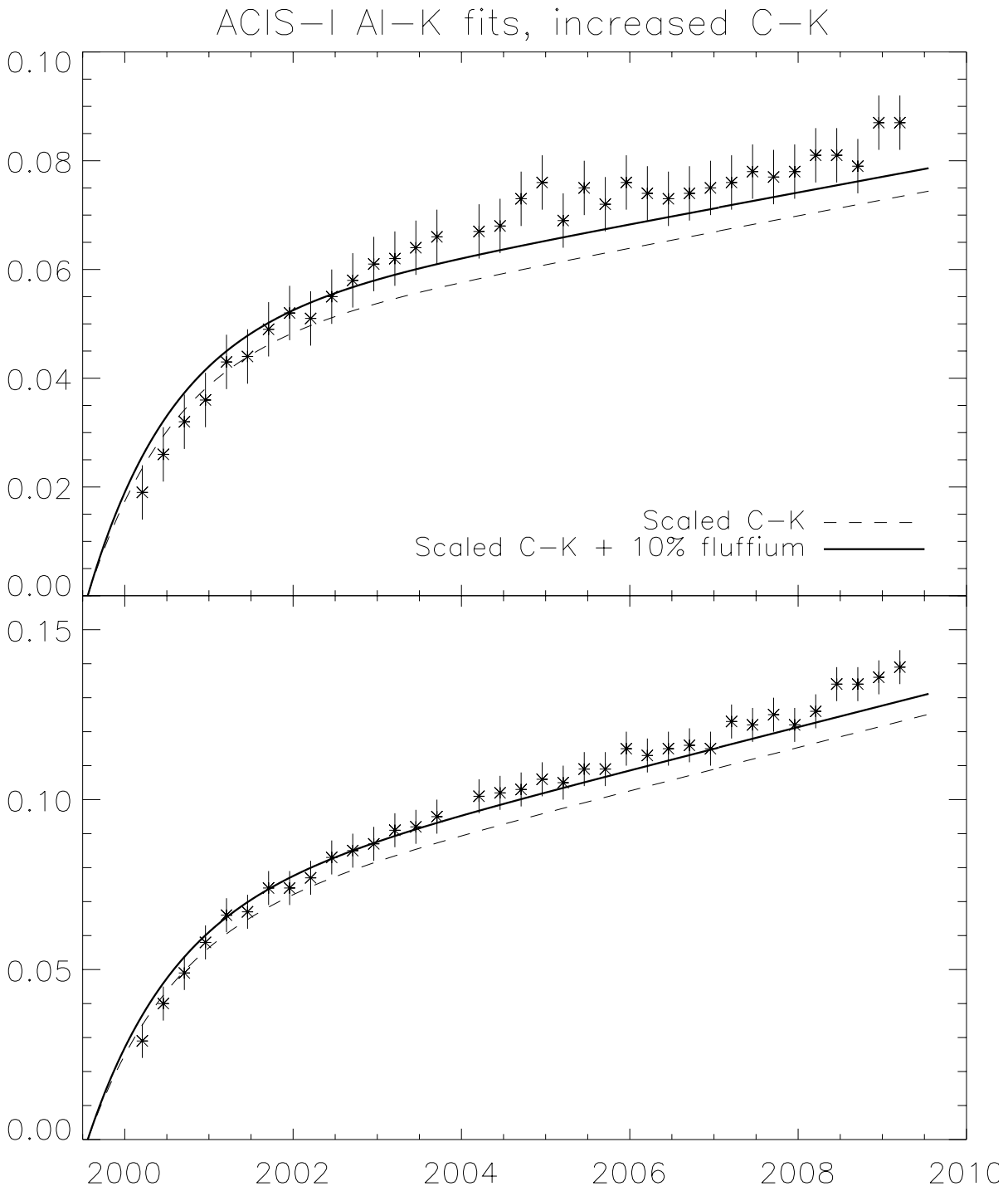


Figure 8: Optical depth at the Al-K $\alpha$  fluorescence line in ECS data at the center (top plot) and periphery (bottom plot) of ACIS-I. The dashed line is the predicted optical depth assuming only absorption by C, O and F. The solid line includes both elemental and fluffium contributions to the total absorption.

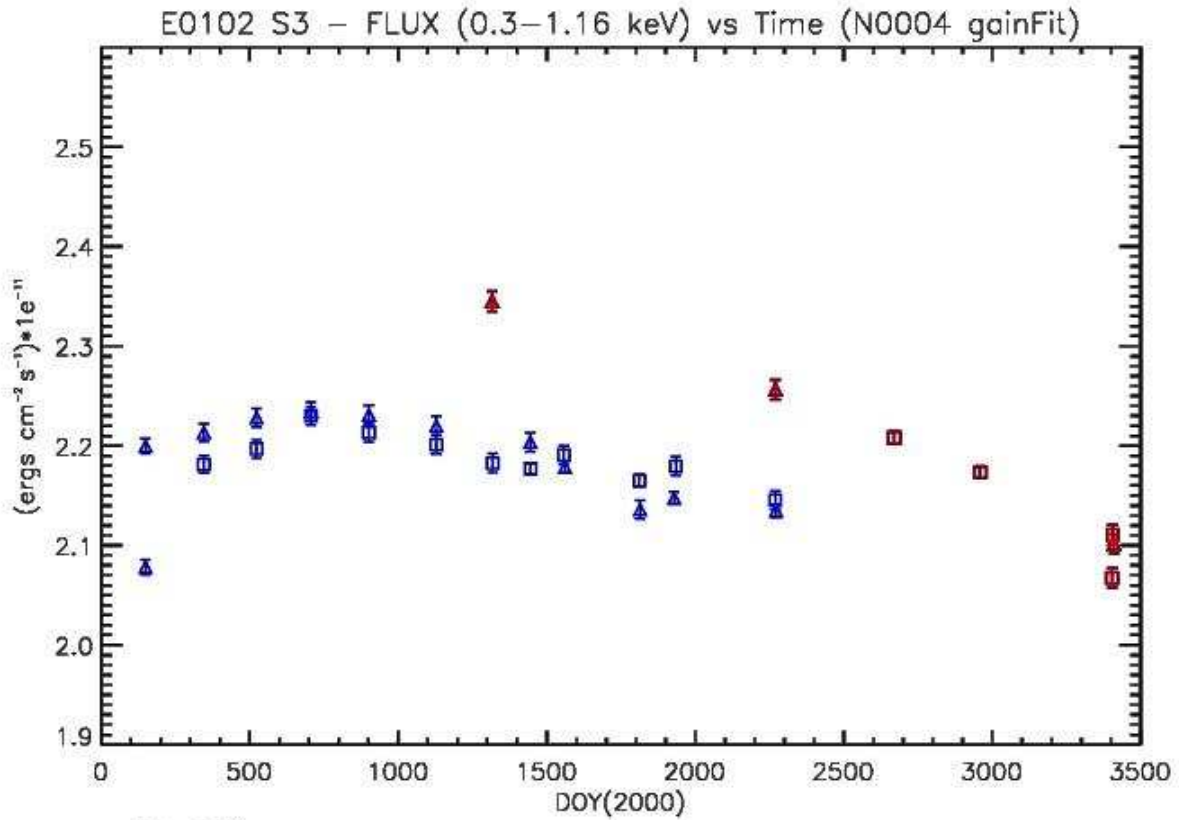


Figure 9: The 0.3-1.16 keV flux in E0102-72 observations derived using version N0004 of the ACIS-S contamination model. The blue data points were done in full-frame mode and the red data points were done with a sub-array. Due to pile-up, the fluxes derived from the sub-array data are slightly higher than those derived from the full-frame data. The square data points refer to observations done on Node 0 of ACIS-S3 and the triangular data points refer to observations done on Node 1 of ACIS-S3. The data point at the lower right was taken toward the read-out where the contamination is thicker.

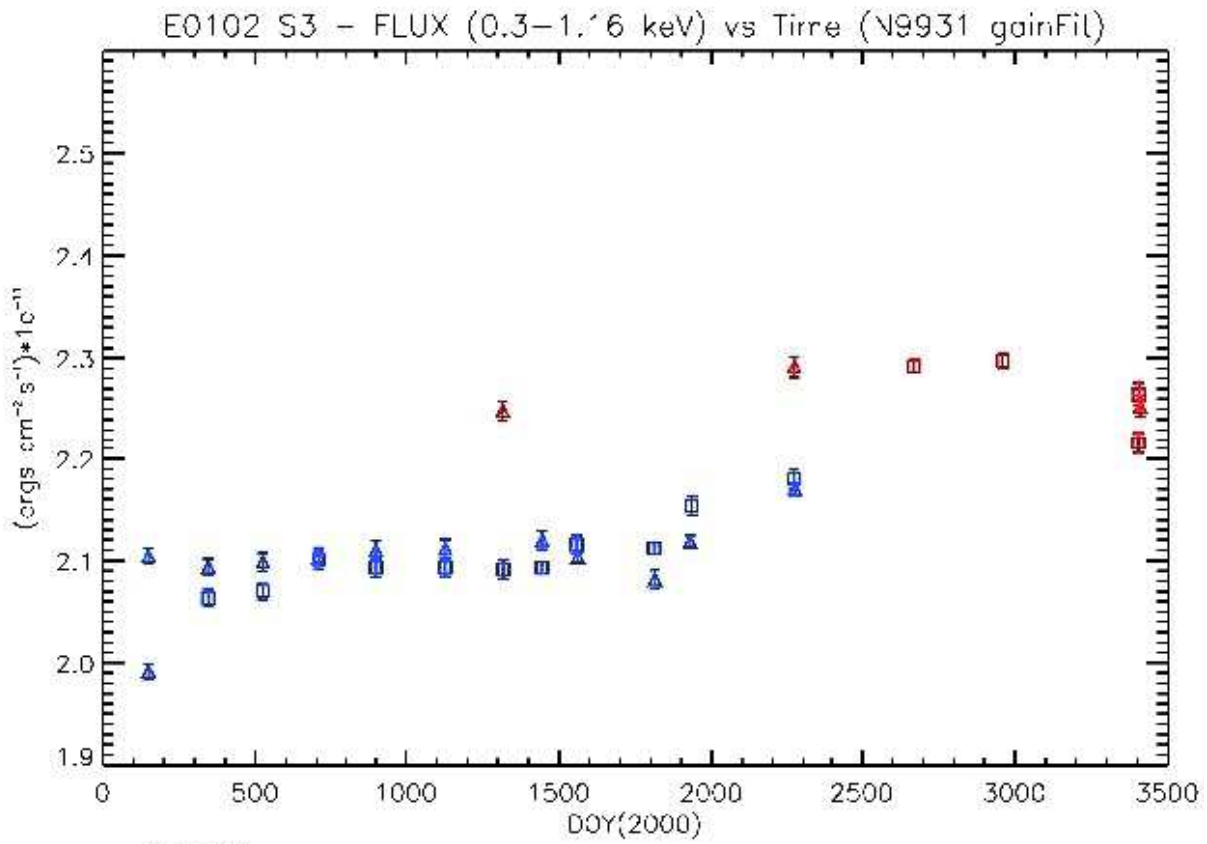


Figure 10: The 0.3-1.16 keV flux in E0102-72 observations derived using version N0005 of the ACIS-S contamination model. The symbols and colors used for the data points are described in the caption to Fig. 9.

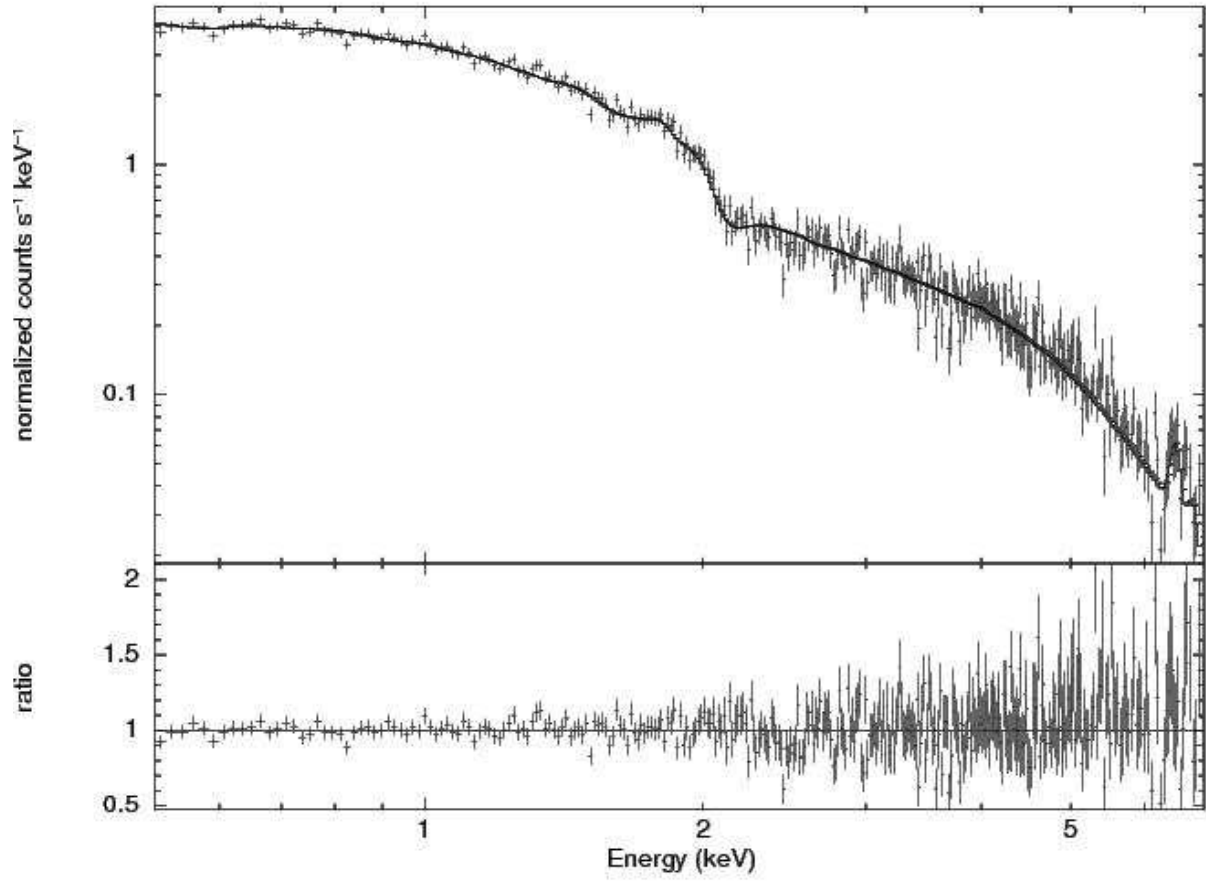


Figure 11: 1999 ACIS-S spectrum of the Coma cluster. The solid curve is the best fit absorbed single temperature model with the absorption fixed to the galactic value.

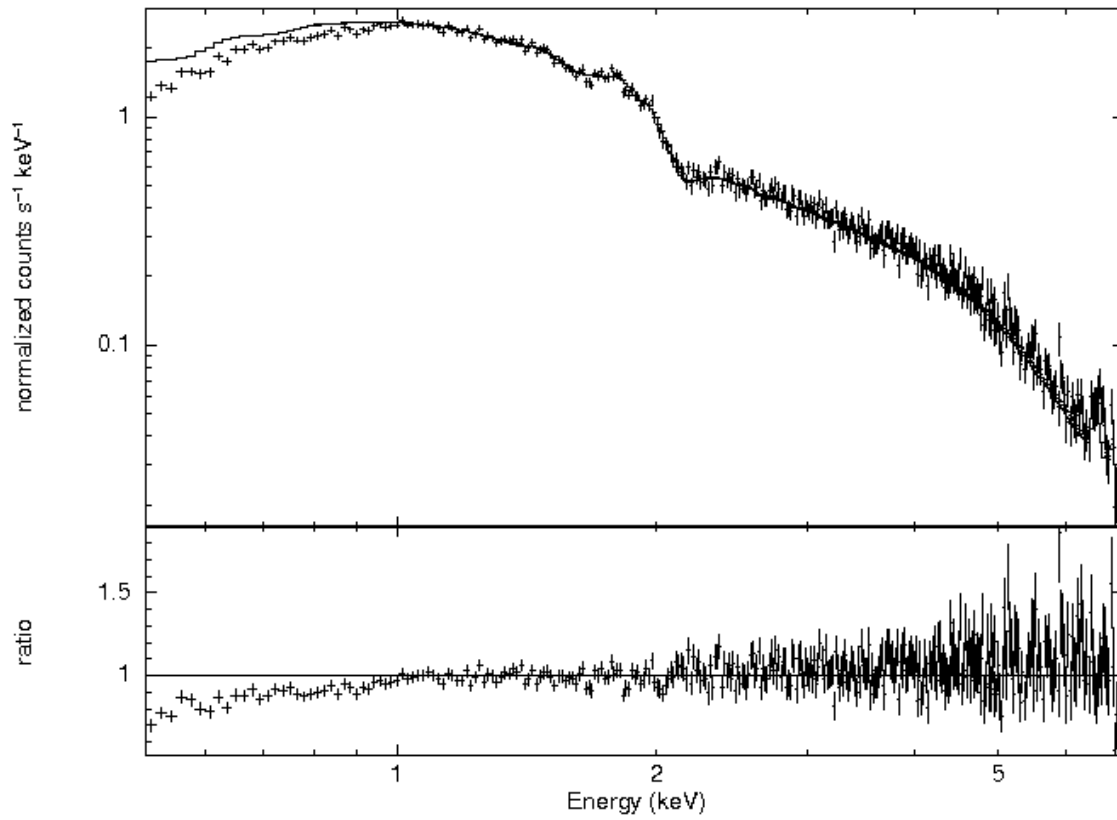


Figure 12: 2009 ACIS-S spectrum of the Coma cluster. The solid curve is the best fit model to the 1999 spectrum using version N0004 the ACIS-S contamination model.

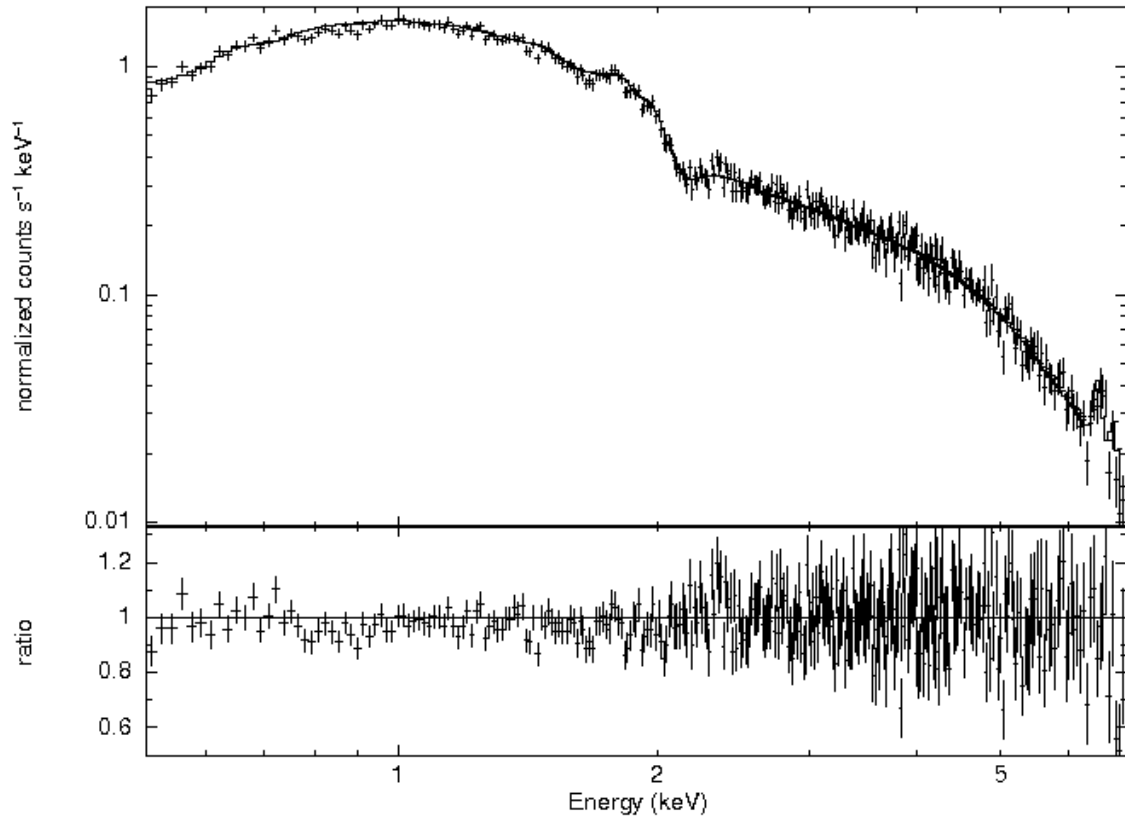


Figure 13: 2009 ACIS-S spectrum of the Coma cluster. The solid curve is the best fit model to the 1999 spectrum using version N0005 the ACIS-S contamination model.

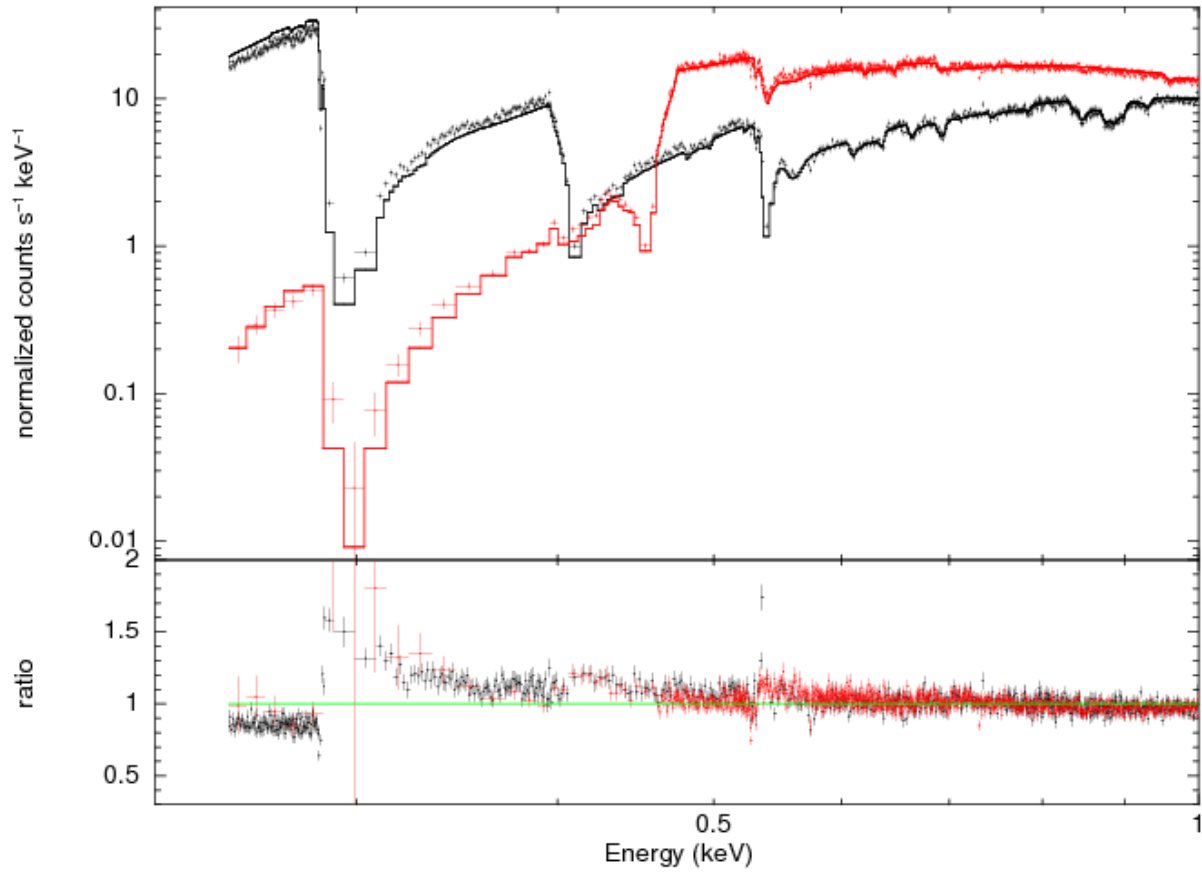


Figure 14: A LETG/ACIS-S spectrum of Mkn421 fitted to an absorbed power-law model using version N0004 of the ACIS contamination model.

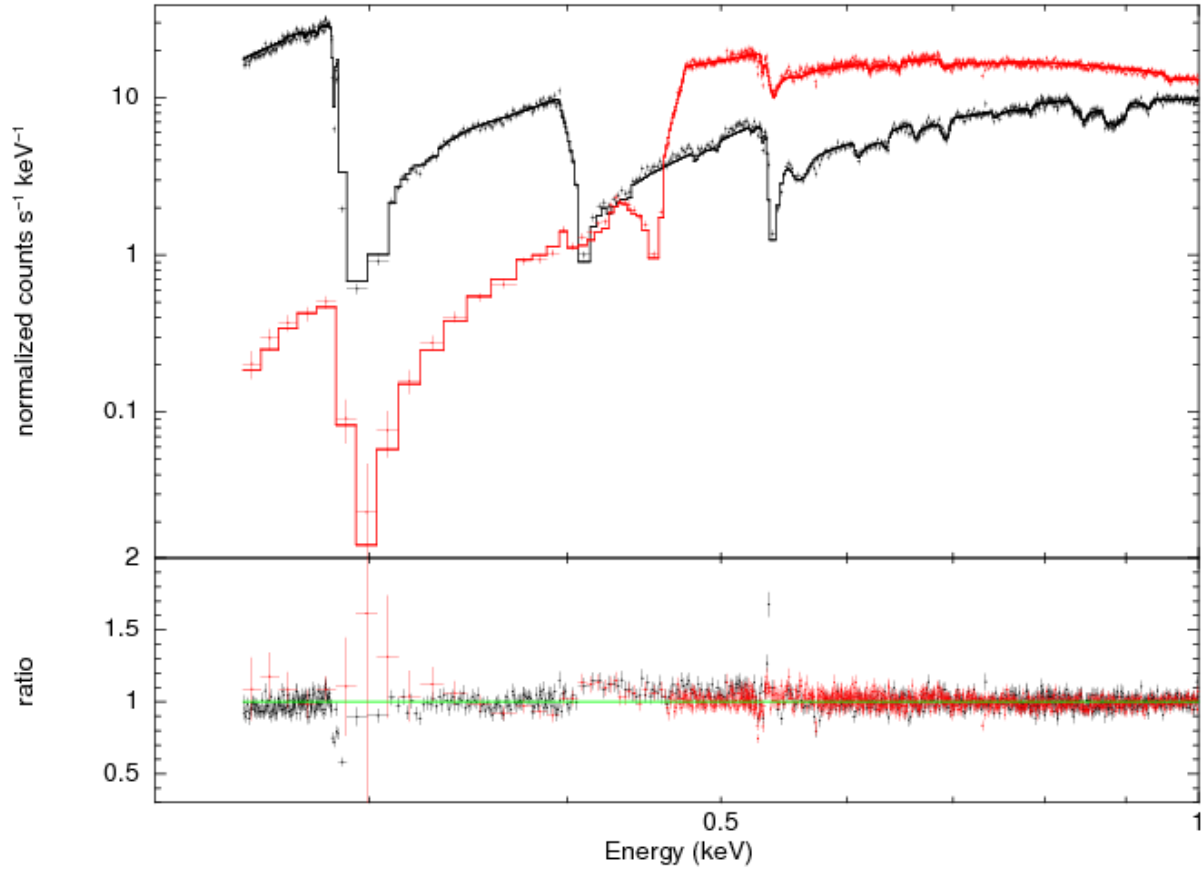


Figure 15: A LETG/ACIS-S spectrum of Mkn421 fitted to an absorbed power-law model using version N0005 of the ACIS contamination model.

Table 1: Clusters of Galaxies

Cluster	ObsId	Date	kT(N0004) (keV)	Flux(N0004) (erg cm <sup>-2</sup> s <sup>-1</sup> )	kT(N0005) (keV)	Flux(N0005) (erg cm <sup>-2</sup> s <sup>-1</sup> )
MKW3s	900	04-03-00	1.30 (1.29-1.31)	1.70e-12	1.28 (1.27-1.29)	1.71e-12
A2199	497	05-13-00	4.32 (4.24-4.40)	1.64e-11	5.07 (4.97-5.17)	1.71e-11
A85	904	08-19-00	5.56 (5.48-5.63)	1.84e-11	6.04 (5.93-6.15)	1.88e-11
A262	2215	08-03-01	2.33 (2.29-2.38)	5.24e-12	2.46 (2.42-2.50)	5.11e-12
A3112	2516	09-15-01	4.97 (4.79-5.16)	8.95e-12	5.45 (5.27-5.64)	8.84e-12
A3571	4203	07-31-03	7.20 (7.03-7.36)	3.65e-11	8.06 (7.81-8.32)	3.60e-11
A2029	4977	01-08-04	7.86 (7.76-7.97)	2.07e-11	8.78 (8.68-8.89)	2.03e-11
Hydra A	4969	01-13-04	3.48 (3.45-3.51)	1.03e-11	3.66 (3.63-3.69)	1.01e-11
A1795	6160	03-20-05	5.74 (5.64-5.85)	1.99e-11	6.34 (6.18-6.51)	1.98e-11
A2052	5807	03-24-06	3.25 (3.22-3.27)	7.23e-12	3.31 (3.28-3.38)	7.12e-12
NGC 5044	9399	03-07-08	3.92 (3.86-3.97)	8.54e-12	3.97 (3.91-4.03)	8.48e-12
Coma	9714	03-20-08	8.34 (8.21-8.46)	6.08e-11	8.76 (8.64-8.89)	6.04e-11

Notes: Spectral analysis results for a sample of 12 groups and clusters. This table gives the best-fit temperatures and 0.5-7.0 keV fluxes, along with their  $1\sigma$  errors, using versions N0004 and N0005 of the ACIS contamination model. All spectra were fit in the 0.5-7.0 keV energy band to an absorbed single temperature model with the absorption fixed at the galactic value.

Table 2: Spectral Fitting Results for a Sample of LETG/ACIS-S AGN Observations

Target	ObsId	Version	Date	$N_{\text{H}}$ ( $10^{20} \text{ cm}^{-2}$ )	$\Gamma_1$ (keV)	$\Gamma_1$ (keV)	$E_j$ (keV)	Flux ( $\text{erg cm}^{-2}\text{s}^{-1}$ )
Ton S180	0811	N0004	12-14-99	$1.000 \pm 0.002$	$1.670 \pm 0.027$	$1.773 \pm 0.040$	$2.374 \pm 0.218$	2286.31+-16.9707
Ton S180	0811	N0005	12-14-09	$1.001 \pm 0.012$	$1.697 \pm 0.023$	$1.741 \pm 0.025$	$2.789 \pm 0.284$	2268.54+-20.6149
3C 273	2471	N0004	6-15-01	$1.000 \pm 0.002$	$0.825 \pm 0.036$	$1.018 \pm 0.062$	$7.894 \pm 0.297$	2463.17+-28.1769
3C 273	2471	N0005	6-15-01	$1.000 \pm 0.001$	$0.842 \pm 0.034$	$0.959 \pm 0.054$	$8.727 \pm 0.266$	2412.88+-24.1516
PKS 2155-304	3668	N0004	6-11-02	$2.068 \pm 0.131$	$1.345 \pm 0.041$	$2.065 \pm 0.052$	$2.875 \pm 0.200$	4874.84+-48.4803
PKS 2155-304	3668	N0005	6-11-02	$1.095 \pm 0.066$	$1.295 \pm 0.036$	$2.030 \pm 0.150$	$4.273 \pm 0.466$	4883.73+-49.8407
Mkn 421	5332	N0004	6-14-04	$2.715 \pm 0.054$	$1.199 \pm 0.008$	$1.512 \pm 0.017$	$7.982 \pm 0.425$	38080.4+-156.357
Mkn 421	5332	N0005	6-14-04	$1.710 \pm 0.053$	$1.147 \pm 0.005$	$1.482 \pm 0.008$	$11.095 \pm 0.239$	39509.5+-209.122
PKS 2155-304	6927	N0004	4-02-06	$1.418 \pm 0.192$	$1.481 \pm 0.081$	$1.934 \pm 0.065$	$1.090 \pm 0.079$	1274.95+-18.9813
PKS 2155-304	6927	N0005	4-02-06	$1.017 \pm 0.040$	$1.782 \pm 0.022$	$1.813 \pm 0.022$	$2.567 \pm 0.929$	1512.99+-24.4194
PKS 2155-304	10662	N0004	5-28-09	$1.010 \pm 0.005$	$1.254 \pm 0.030$	$2.551 \pm 0.067$	$2.691 \pm 0.291$	3905.60+-34.3020
PKS 2155-304	10662	N0005	5-08-29	$1.004 \pm 0.012$	$1.597 \pm 0.088$	$2.069 \pm 0.176$	$3.138 \pm 0.810$	5235.47+-64.9737

Notes: Spectral fitting results for a sample of AGN using versions N0004 and N0005 of the ACIS contamination model. All spectra were fit to a reciprocal joint power-law model ( $1/(a_1 E^{\gamma_1} + a_2 E^{\gamma_2})$ ) where  $a_2 = a_1 E_j^{(\gamma_1 - \gamma_2)}$ .